Spindle positioning in human cells relies on proper centriole formation and on the microcephaly proteins CPAP and STIL

Daiju Kitagawa*, Gregor Kohlmaier, Debora Keller, Petr Strnad‡, Fernando R. Balestra, Isabelle Flückiger and Pierre Gönczy§

Swiss Institute for Experimental Cancer Research (ISREC), School of Life Sciences, Swiss Federal Institute of Technology (EPFL), Lausanne, Switzerland

*Present address: Center for Frontier Research, National Institute of Genetics, Mishima, Japan
‡Present address: European Molecular Biology Laboratory (EMBL), Heidelberg, Germany
§Author for correspondence (Pierre.Gonczy@epfl.ch)

Accepted 18 July 2011
Journal of Cell Science 124, 3884–3893

doi: 10.1242/jcs.089888

Summary

Patients with MCPH (autosomal recessive primary microcephaly) exhibit impaired brain development, presumably due to the compromised function of neuronal progenitors. Seven MCPH loci have been identified, including one that encodes centrosome protein 4.1 associated protein (CPAP; also known as centromere protein J, CENPJ). CPAP is a large coiled-coil protein enriched at the centrosome, a structure that comprises two centrioles and surrounding pericentriolar material (PCM). CPAP depletion impairs centriole formation, whereas CPAP overexpression results in overly long centrioles. The mechanisms by which CPAP MCPH patient mutations affect brain development are not clear. Here, we identify CPAP protein domains crucial for its centriolar localization, as well as for the elongation and the formation of centrioles. Furthermore, we demonstrate that conditions that resemble CPAP MCPH patient mutations compromise centriole formation in tissue culture cells. Using adhesive micropatterns, we reveal that such defects correlate with a randomization of spindle position. Moreover, we demonstrate that the MCPH protein SCL/TAL1 interrupting locus (STIL) is also essential for centriole formation and for proper spindle position. Our findings are compatible with the notion that mutations in CPAP and STIL cause MCPH because of aberrant spindle positioning in progenitor cells during brain development.

Key words: CPAP, Centriole formation, Microcephaly, Spindle positioning

Introduction

Autosomal recessive primary microcephaly (MCPH) is a severe congenital disorder characterized by a small brain size and associated mental retardation (reviewed by Thornton and Woods, 2009). It is thought that MCPH results from defects in the neuroepithelial progenitor cells located in the ventricular zone of the developing neocortex. Early in normal brain development, these progenitors undergo symmetrical divisions in which the spindle is usually positioned parallel to the ventricular surface. This can generate two daughter cells that retain progenitor fate and sustain lateral expansion of the developing brain. Later, these progenitors undergo asymmetrical divisions in which spindle position is typically perpendicular to the ventricular surface. This can give rise to one daughter cell that maintains contact with the ventricular zone and retains the progenitor fate, and the other daughter that adopts a neuronal fate. Despite a smaller brain size, the overall organization of the neocortex is not altered in MPCH patients, suggesting that it is the initial stage of lateral expansion that is somehow defective (reviewed by Thornton and Woods, 2009).

Analyses of affected families have led to the identification of seven loci that, when mutated, cause MCPH (reviewed by Thornton and Woods, 2009). Most of these loci encode proteins enriched at centrosomes, indicating that MCPH might stem from defective microtubule-dependent processes. Accordingly, in the developing mouse brain, RNA interference (RNAi)-mediated depletion of the homologue of the MCPH5 component abnormal spindle-like microcephaly-associated protein (ASPM) results in defective spindle positioning and decreased progenitor number (Fish et al., 2006). Moreover, depletion of ASPM in human cells leads to severe defects during mitosis, including in spindle positioning (Higgins et al., 2010). Whereas ASPM proteins serve to focus spindle microtubules (Wakefield et al., 2001), other MCPH proteins exert distinct cellular functions (reviewed by Thornton and Woods, 2009). Therefore, it remains to be determined whether mistakes in spindle positioning might offer a unifying theme for the root of MCPH.

The locus *MCPH6* (also known as *CENPJ*, centromere protein J) encodes CPAP (Bond et al., 2005), a protein that is enriched at centrosomes and also present in the cytoplasm of proliferating cells (Hung et al., 2000; Kohlmaier et al., 2009; Schmidt et al., 2009; Tang et al., 2009). CPAP is related to SAS-4, a protein originally identified in *C. elegans* as being required for centriole formation (Kirkham et al., 2003; Leidel and Gönczy, 2003). Likewise, CPAP is essential for centriole formation in human cells, and its overexpression generates overly long centrioles that exhibit branched structures and interfere with cell division (Kohlmaier et al., 2009; Schmidt et al., 2009; Tang et al., 2009).

Journal of Cell Science

In *Drosophila*, homozygous mutant Sas-4 animals are viable owing to the persistence of maternal stores, but exhibit several phenotypes, including abnormal division of larval neuroblasts (Basto et al., 2006).

Human CPAP is 1338 amino acids long and harbors four coiled-coil motifs predicted by SMART (http://smart.embl-heidelberg.de/), as well as a C-terminal TCP domain related to the t-complex 10 protein (Fig. 1A). CPAP also has a so-called PN2-3 domain that binds tubulin dimers and is important for centriole elongation (Fig. 1A) (Cormier et al., 2009). The PN2-3 domain encompasses the region most conserved between CPAP and SAS-4, which we named the SAC-box (for 'similar in SAS-4 and CPAP'; supplementary material Fig. S1). The three known MCPH familial mutations in the CPAP gene are schematized in Fig. 1A. Two of these are premature stop codons predicted to severely truncate the protein (M1) or to result in a protein lacking the TCP domain (M2) (Bond et al., 2005; Gul et al., 2006). The third familial mutation (M3) is an E1235V missense mutation within the TCP domain (Bond et al., 2005). How the different domains of CPAP contribute to its function is incompletely understood, and importantly, how MCPH patient mutant variants of CPAP might affect cell division and ultimately result in the depletion of progenitor cells is not understood.

Results

CPAP localizes primarily to centrioles and exchanges with the cytoplasmic pool

We conducted immunofluorescence analysis in U2OS cells to determine the exact distribution of CPAP at centrosomes. We found that during interphase, CPAP overlaps partially with the centriolar component centrin-1 and the PCM component γ-tubulin (Fig. 1B, top). During mitosis, the CPAP signal is much more focused than γ-tubulin (Fig. 1B, bottom), indicating that CPAP is enriched primarily at centrioles. We located more precisely where CPAP resides by conducting triple-labeling experiments and found that the center of the CPAP signal is located mid-way between the C-Nap1 and centrin-1 signals (Fig. 1C,D; supplementary material Movie 1), which mark the centriole proximal and distal ends, respectively (Fry et al., 1998; Piel et al., 2000). This is in line with immuno-electron microscopy experiments conducted in cells with supernumerary centrioles upon overexpression of the Polo-like kinase Plk4 (Kleylein-Sohn et al., 2007) and indicates that CPAP is enriched primarily in the center of the centriolar cylinder.

We set out to address whether centrosomal CPAP exchanges with the cytoplasmic pool. To this end, we conducted fluorescence recovery after photobleaching (FRAP) experiments with cells depleted of endogenous CPAP, using short interfering RNAs (siRNAs), and induced to express GFP–CPAP resistant to these siRNAs (Fig. 1E, Fig. 2A) (Kohlmaier et al., 2009). We found that ~50% of the centrosomal GFP–CPAP signal recovers within 6 minutes after photobleaching (Fig. 1F), suggesting that centrosomal CPAP readily exchanges with the cytoplasmic pool of the protein. Given that there is approximately five times more GFP–CPAP in these cells than there is endogenous CPAP in control cells (data not shown), we cannot exclude that this recovery profile is due in part to having excess protein. Regardless, additional FRAP experiments with cells expressing GFP–CPAP as well as endogenous CPAP established that the kinetics of centriolar recovery is indistinguishable in the G1, S and G2 phases of the cell cycle (Fig. 1G) and that ~80% of the GFP–CPAP centriolar signal recovers within an hour (Fig. 1H).

Overall, we conclude that CPAP resides at or very near centrioles and appears to be able to readily exchange with a cytoplasmic pool throughout the cell cycle.

MCPH patient variants alter the function of CPAP in centriole elongation

How the different domains of CPAP contribute to centriolar localization and to the ability to generate overly long centrioles when overexpressed is incompletely understood. To address these questions, we depleted endogenous CPAP using siRNAs and expressed RNAi-resistant mutant and deletion constructs tagged with GFP at comparable levels (Fig. 2A; supplementary material Fig. S2). We found that expression of GFP-tagged full-length CPAP resulted in overly long centrioles in 38% such cells (Fig. 2B–D). By contrast, proteins lacking the PN2-3 or the SAC domain, although still localizing to centrioles, were dramatically impaired in their ability to induce overly long centrioles (Fig. 2C,D). We conclude that these domains are crucial for centriole elongation. In addition, a protein lacking the fourth coiled-coil domain (CC4) did not localize to centrioles and failed to induce overly long centrioles (Fig. 2C,D). Moreover, we found that CC4 is sufficient for centriolar targeting (supplementary material Fig. S3). These results lead us to conclude that CPAP centriolar localization is mediated primarily by CC4.

Using the same experimental approach, we engineered expression of CPAP to resemble the three MCPH patient mutations: siRNA-mediated depletion of CPAP, which resembles mutation M1, expression of a ΔTCP construct lacking the TCP domain, which resembles mutation M2, and expression of a full-length protein harboring the E1235V point mutation M3. We found that cells depleted of CPAP or expressing solely the ΔTCP protein did not promote the formation of overly long centrioles (Fig. 2B–D). By contrast, overly long centrioles were more numerous and longer on average upon expression of the E1235V construct compared with wild-type full-length CPAP (Fig. 2C,D; supplementary material Fig. S4A). Moreover, the branching pattern of overly long centrioles induced by E1235V was more pronounced (supplementary material Fig. S4B,C). Overall, these findings indicate that E1235V is more potent in promoting centriole elongation than wild-type CPAP. Given that overly long centrioles can interfere with proper cell division (Kohlmaier et al., 2009), this raises the possibility that defective division of neuroepithelial progenitors is more frequent in patients expressing this mutant protein.

MCPH patient variants affect CPAP function in centriole formation

We next investigated which domains of CPAP are important for centriole formation, using the same experimental strategy. We analyzed cells in mitosis, which normally have four centrioles and assemble a bipolar spindle (Fig. 3A–D). Upon depletion of endogenous CPAP, most mitotic cells had ≤2 centrioles and assembled a monopolar spindle (Fig. 3A–D) (Kohlmaier et al., 2009; Schmidt et al., 2009; Tang et al., 2009). We found that only a minority of mitotic cells depleted of endogenous CPAP and expressing the siRNA-resistant full-length protein had ≤2 centrioles and assembled a monopolar spindle, indicating functional rescue (Fig. 3A–D). By contrast, expression of fusion

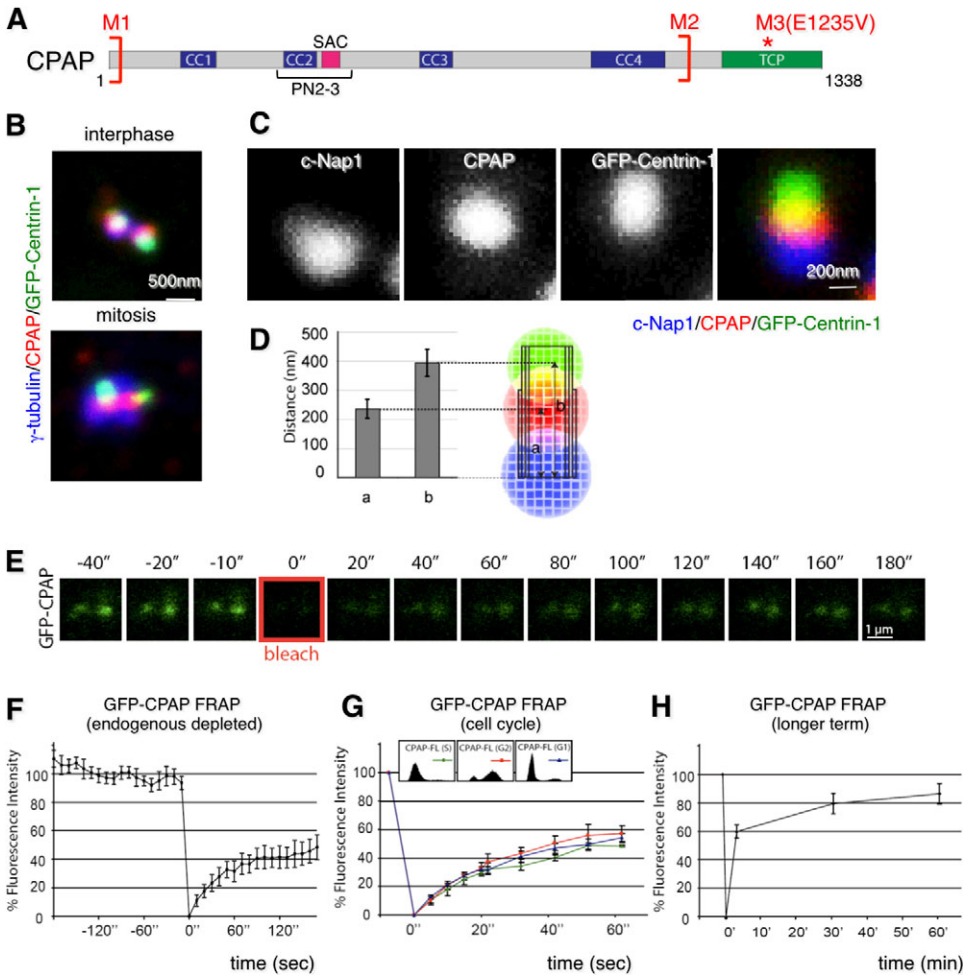

Fig. 1. CPAP distribution and dynamics. (**A**) Schematic representation of CPAP protein. The four coiled-coil (CC) domains are represented in blue (CC1: aa 142–186, CC2: 339–360, CC3: 556–580 and CC4: 899–1047), the TCP domain in green, the PN2-3 domain (aa 311–422) by a bracket, and the SAC-box (aa 370–385) in pink. The position of the three MCPH mutations is indicated: M1: T6fsX3, single base-pair deletion 17delC; M2: four base-pairs deletion 3243–3246delTCAG; M3: E1235V, missense mutation A3704T. M1 and M2 are predicted to encode truncated proteins, as schematized by the vertical brackets. Note that these truncated proteins might not be present at normal levels owing to degradation of the corresponding mRNAs by nonsense mediated decay. (**B**) U2OS cells in interphase (top) or mitosis (bottom) expressing GFP–centrin-1 and stained with antibodies against γ-tubulin (blue), CPAP (red) and GFP (green). For mitosis, only one spindle pole is shown. Identical results were obtained using a distinct CPAP antibody (data not shown). (**C**) U2OS cells expressing GFP–centrin-1 stained with antibodies against C-Nap1 (blue in the merge), CPAP (red in the merge) and GFP (green in the merge). (**D**) Distances between the center of C-Nap1 and CPAP or the center of C-Nap1 and GFP signals (see C) were measured for 20 interphase centrioles and mapped onto a virtual centriole with dimensions 450 × 150 nm. Error bars represent standard deviations. The values a and b are significantly different from one another (two-tailed Student's *t*-test, $P<0.05$). (**E**) Illustration of FRAP experiment shown in F. (**F**) Centriole-associated fluorescence signal in U2OS cells treated for 48 hours with siRNA against endogenous CPAP and induced to express a GFP–CPAP RNAi-resistant construct. Seven cells were recorded for 3 minutes before and for 3 minutes after photobleaching. Error bars represent 95% confidence intervals at each time point (also in G and H). In F, 100% fluorescence intensity corresponds to the average of the values in the 3 minutes preceding photobleaching, 0% to the value in the first image following photobleaching. Note that there appeared to be a tendency for those cells expressing lower levels of GFP–CPAP to exhibit slower recovery profiles. (**G**) Recovery of centriole-associated fluorescence signal in HeLa cells synchronized, analyzed by FACS as indicated (G1, purple; S phase, green; G2, red) and transiently transfected for 24 hours with GFP–CPAP. In G and H, 100% fluorescence intensity corresponds to the value in the last image before photobleaching, 0% to that in the first image following photobleaching. (**H**) Recovery of centriole-associated fluorescence signal in U2OS cells induced to express GFP–CPAP. Cells were recorded for 3 minutes before and at 3, 30 and 60 minutes after photobleaching. $n=7$ cells.

proteins lacking the PN2-3, the SAC or the CC4 domain failed to rescue centriole formation and bipolar spindle assembly (Fig. 3A–D). Therefore, these domains are necessary for centriole formation. In addition, expression of the ΔTCP construct failed to rescue centriole formation and bipolar spindle assembly, whereas the E1235V construct rescued these phenotypes to a lesser extent than wild-type full-length CPAP (Fig. 3A–D). The fact that E1235V was more active in inducing overly long centrioles while being slightly compromised for centriole formation indicates that these two functions of CPAP can be separated.

Overall, these findings indicate that the three conditions that resemble CPAP MCPH patient mutations are severely (CPAP siRNA and ΔTCP) or slightly (E1235V) compromised in their centriole formation activity.

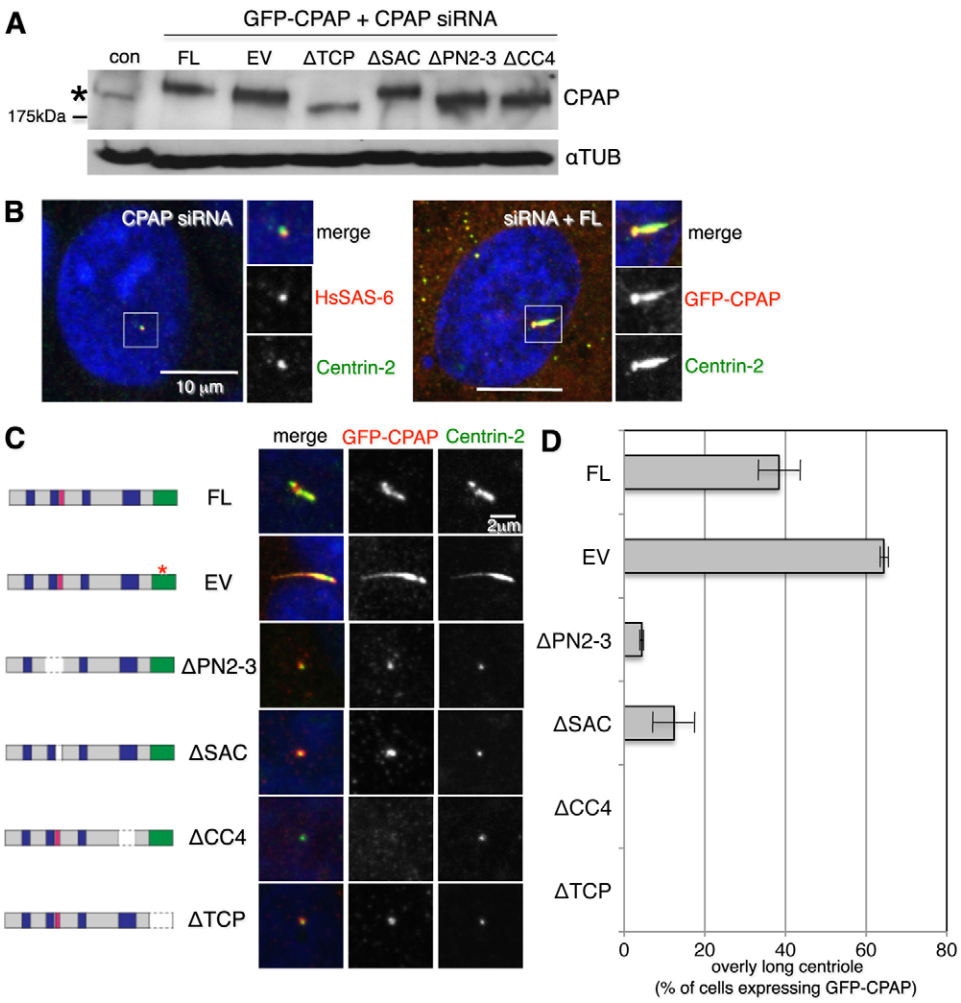

Fig. 2. CPAP domains required for centriole elongation. (**A**) Control U2OS cells, or U2OS cells expressing RNAi-resistant constructs for GFP fused to CPAP full-length wild-type (FL), full-length E1235V (EV), ΔTCP, ΔSAC, ΔPN2-3 or ΔCC4, as indicated, treated with siRNA against endogenous CPAP and analyzed by western blotting using antibodies against CPAP or α-tubulin as a loading control. The asterisk indicates endogenous CPAP in control cells. Note that endogenous CPAP is not detectable in all other lanes, whereas the RNAi-resistant constructs are expressed. (**B**) Control U2OS cell (left) or U2OS cell expressing RNAi-resistant GFP–CPAP full-length (FL) and treated with siRNAs against endogenous CPAP were stained with antibodies against HsSAS-6 or GFP, as indicated (both in red), as well as centrin-2 (green); DNA is shown in blue. Insets show approximately twofold magnified views of spindle poles. (**C**) Schematic representation of CPAP constructs and representative high-magnification views of centrioles in U2OS cells depleted of endogenous CPAP and expressing the following RNAi-resistant CPAP constructs fused to GFP: full-length wild-type (FL), full-length E1235V (EV), ΔPN2-3, ΔSAC, ΔCC4 or ΔTCP. Cells were stained with antibodies against GFP (red) and centrin-2 (green); DNA is shown in blue. (**D**) Frequency of elongated centrioles in cells treated as in B. Values are mean percentages ± s.e.m. from two independent experiments (n>200 for each condition). Means are: 38% (FL), 64% (EV), 4% (ΔPN2-3), 12% (ΔSAC), 0% (ΔCC4), 0% (ΔTCP).

Asymmetrical spindle assembly upon compromised CPAP function

How could defective centriole formation cause impaired brain development in CPAP MCPH patients? One possibility is that defective centriole formation results in aberrant spindle positioning in progenitor cells of the ventricular zone in the developing human neocortex. By analogy with the situation upon acute depletion of ASPM in the mouse (Fish et al., 2006), this could compromise the progenitor pool during the early stages of brain development.

To investigate the possibility that spindle positioning is aberrant in human cells when CPAP function is compromised, we first examined the nature of the mitotic spindles assembled upon CPAP depletion (see also Kohlmaier et al., 2009). For these experiments, we used HeLa cells, which adhered better to printed patterns of fibronectin (see below). In control cells, successful centriole formation results in the presence of four centrioles during mitosis, two per spindle pole (Fig. 4A, control). The two spindle poles of control cells have PCMs of comparable sizes, which direct assembly of a bipolar spindle and nucleate similar arrays of astral microtubules (Fig. 4A–C, control). The failure of centriole formation provoked by siRNA-mediated depletion of CPAP initially led to the presence of two centrioles during mitosis, one per spindle pole (Fig. 4A, symmetric). Such cells had two equal sized regions of PCM and assembled a bipolar spindle indistinguishable from control cells, with symmetrical arrays of astral microtubules (Fig. 4A–C, symmetric). Some affected cells, presumably at subsequent cell cycles following depletion, had one spindle pole with a centrin-3 focus of normal size and intensity and the other one with either no detectable centrin-3 (Fig. 4A, asymmetric) or a smaller and weaker centrin-3 focus (data not shown). This subset of cells assembled an asymmetrical bipolar spindle, whereby the distance between the chromosomes and the spindle pole was shorter on the side of the undetectable or smaller centrin-3 focus (Fig. 4A, asymmetric). As anticipated from centrioles being important for PCM recruitment (Bobinnec et al., 1998), the PCM was also asymmetrical in such cells (Fig. 4B, asymmetric). The same is true of astral microtubules, which were less pronounced on the side of the smaller spindle pole (Fig. 4C, asymmetric). Other cells depleted of CPAP that had a single centriole assembled a monopolar spindle (Fig. 4A, monopolar), which might resolve over time into an asymmetrical spindle with no detectable centrin-3 signal on one side. As reported in Table 1, asymmetrical spindles were present not only in cells depleted of CPAP (resembling M1), but also in those expressing the ΔTCP construct (resembling M2) or the E1235V construct (resembling M3), although their incidence was somewhat lower in the latter case, mirroring the fact that centriole formation was compromised to a lesser extent.

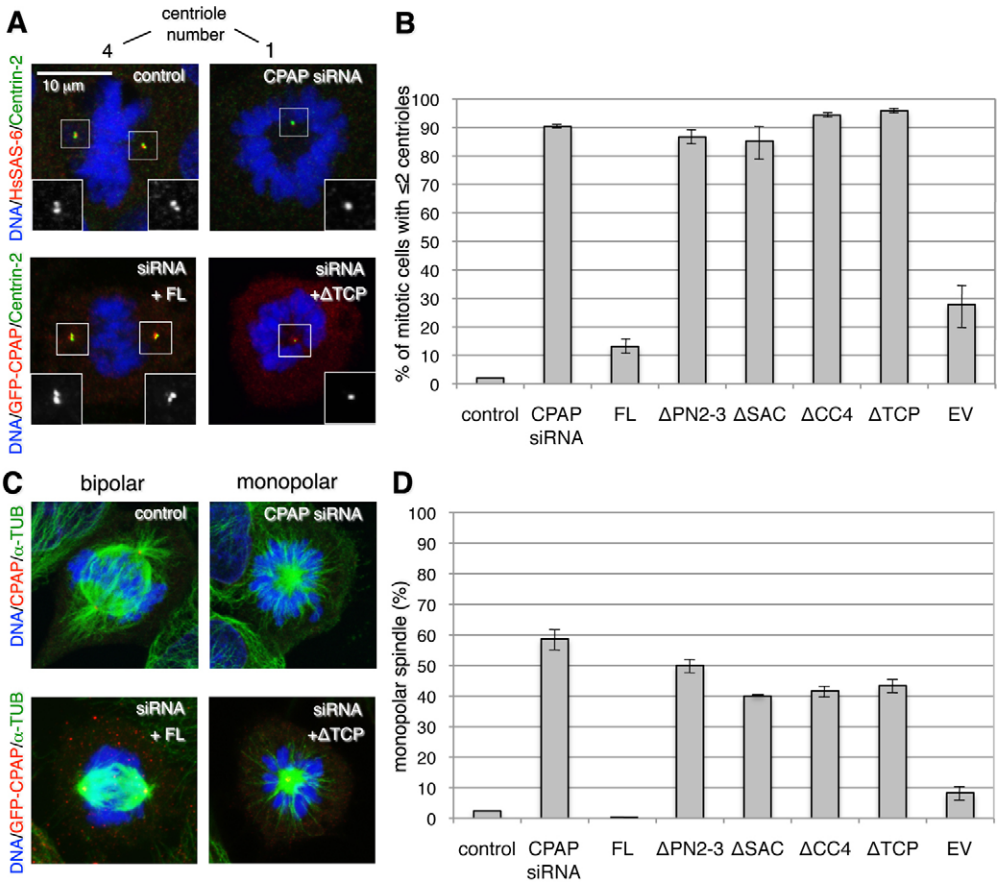

Fig. 3. CPAP domains required for centriole formation. (**A–D**) Control U2OS cells or U2OS cells treated with CPAP RNAi and expressing the indicated RNAi-resistant constructs fused to GFP were stained with antibodies against GFP, HsSAS-6 or CPAP, as indicated (all in red), and against centrin-2 (green in A) or α-tubulin (green in C); DNA is shown in blue. (A) Four representative mitotic cells with the indicated number of centrioles. Insets show approximately twofold magnified views of centrin-2 signals. (B) Frequency of mitotic cells with two or fewer centrioles (for all cell lines, $n \geq 70$ from three independent experiments, except for control cells, where $n=100$ from one experiment, as well as CPAP siRNA cells, where $n=52$ from two independent experiments). (C) Four representative mitotic cells with bipolar or monopolar spindle assembly. (D) Frequency of mitotic cells with monopolar spindle (for all cell lines, $n \geq 60$ from two independent experiments, except for control cells, where $n=100$ from one experiment, and CPAP siRNA cells, where $n=85$ from two independent experiments).

Defective spindle positioning upon compromised CPAP function

Vertebrate cells entirely lacking astral microtubules exhibit defective spindle positioning (Khodjakov and Rieder, 2001; O'Connell and Wang, 2000). We reasoned that spindle positioning might be also affected in human cells with asymmetrical astral microtubules that stem from defects in centriole formation provoked by CPAP depletion or expression of CPAP MCPH mutant proteins. To test this hypothesis, we utilized microfabricated chips in which a printed pattern of fibronectin such as an L-shape directed adhesion of cells to the substrate during interphase (Fig. 5A). This imparted spatial landmarks that allowed astral microtubules to direct spindle positioning in a stereotyped manner during mitosis (Fig. 5B,C) (Théry et al., 2005). In the vast majority of control cells plated on such microfabricated chips, the spindle was positioned along the hypotenuse of the L-shape (Fig. 5D). As mentioned above, most cells depleted of CPAP assemble a monopolar spindle, thus preventing an assessment of spindle positioning in such cases (see supplementary material Fig. S5). However, a sizeable fraction of cells depleted of CPAP assembled a bipolar spindle, which can be symmetrical or asymmetrical (see Table 1). We found that whereas spindle position is analogous to control cells in the subset of CPAP-depleted cells with a symmetrical bipolar spindle (Fig. 5E; supplementary material Fig. S6A), spindle position is randomized in those cells with an asymmetrical bipolar spindle (Fig. 5F; supplementary material Fig. S6A). Thus, depleting CPAP leads to severe spindle positioning defects.

We then investigated whether spindle positioning is defective in the other two conditions resembling CPAP MCPH patient mutations. We verified that cells depleted of endogenous CPAP and expressing RNAi-resistant full-length CPAP usually assemble a symmetrical bipolar spindle and undergo spindle positioning in a manner indistinguishable from that of control cells (Fig. 5G; supplementary material Fig. S6A; Table 1). By contrast, we found that spindle positioning is severely impaired in those cells expressing solely the ΔTCP or the E1235V constructs and assembling an asymmetrical bipolar spindle (Fig. 5H,I; supplementary material Fig. S6A).

Taken together, our findings raise the possibility that the mutations of CPAP in MCPH patients impair brain development as a result of aberrant spindle positioning due to defective centriole formation in progenitor cells.

Proper centriole formation is crucial for spindle positioning in human cells

We set out to determine whether spindle positioning defects deriving from impaired centriole formation could explain the phenotype associated with other MCPH loci. For this analysis, we selected the locus *MCPH7*, which encodes the centrosomal protein SCL/TAL1 interrupting locus (STIL) (Kumar et al., 2009). It has been suggested that STIL is related to *C. elegans* SAS-5 and *Drosophila* Ana2 (Stevens et al., 2010a), both of which are essential for centriole formation (Dammermann et al., 2004; Delattre et al., 2004; Stevens et al., 2010a). However, whether STIL is required for centriole formation in human cells

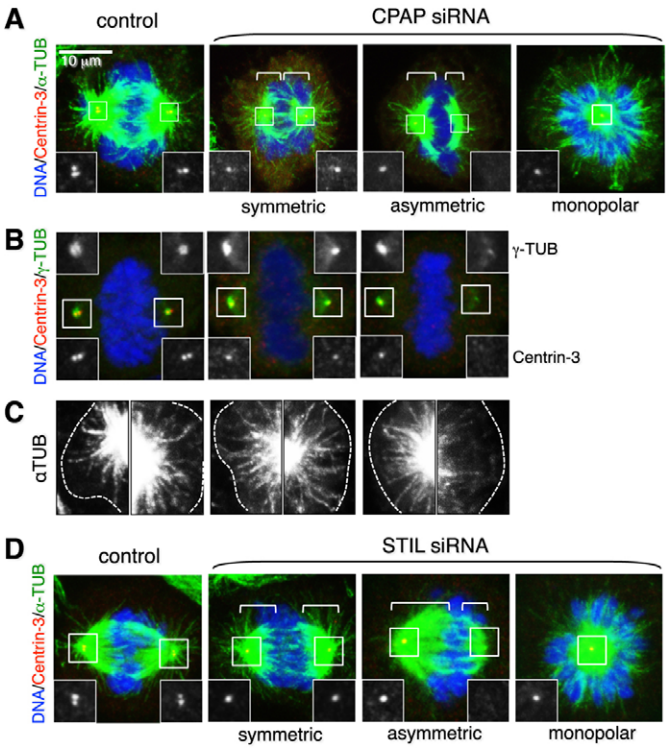

Fig. 4. Asymmetrical spindle assembly upon compromised CPAP or STIL function. (**A**,**B**) Mitotic control HeLa cells or HeLa cells treated with CPAP siRNAs stained with antibodies against α-tubulin (A) or γ-tubulin (B) (both in green) and centrin-3 (red); DNA is shown in blue. Insets show approximately twofold magnified views of spindle poles. The text between panels A and B indicates the category of mitotic spindles. Brackets in the two central panels denote the distance between chromosomes and spindle poles. Note that cells treated with CPAP siRNAs and assembling an asymmetrical spindle always exhibited an asymmetry between the two spindle poles as judged by unequal centrin-3 or γ-tubulin signals ($n=16$); the same was true of cell treated with STIL siRNAs (see D; $n=10$). (**C**) Magnified view of astral microtubules emanating from the spindle poles of the three cells assembling a bipolar spindle that are shown in A. The central portion of the cell is not shown. (**D**) Control mitotic HeLa cells or HeLa cells treated with STIL siRNAs stained with antibodies against α-tubulin (green) and centrin-3 (red); DNA is shown in blue. Insets show ~1.5-fold magnified views of spindle poles. The text below the panels indicates the category of mitotic spindles. Brackets in the two central panels denote the distance between chromosomes and spindle poles.

has not been addressed. As shown in Fig. 4D and supplementary material Fig. S7, we found that siRNA-mediated depletion of STIL resulted in a failure of centriole formation, with mitotic cells that had usually ≤2 centrin-3-positive foci instead of the usual four, as is the case for cells depleted of CPAP (see Fig. 4A). A similar failure of centriole formation was observed using two distinct siRNAs directed against STIL (data not shown). We conclude that STIL is required for centriole formation in human cells. Furthermore, we found again that some affected cells assembled an asymmetrical bipolar spindle in which less pronounced astral microtubules emanated from one spindle pole (Fig. 4D, asymmetric; Table 1). Importantly, we also found that whereas spindle position was normal in those STIL-depleted cells with a symmetrical bipolar spindle (Fig. 6A; supplementary material Fig. S6B), spindle position was randomized in the subset of cells with asymmetrical spindles (Fig. 6B; supplementary material Fig. S6B). Therefore, STIL is also crucial for proper spindle positioning in human cells.

To address more generally whether spindle positioning defects are a systematic consequence of compromised centriole formation in human cells, we conducted analogous experiments in cells depleted of human-SAS-6 (HsSAS-6), which, although not an identified MCPH locus, is also essential for centriole formation (Strnad et al., 2007). In this case as well, spindle positioning was indistinguishable from control conditions in the subset of cells with a symmetrical bipolar spindle (Fig. 6C; supplementary material Fig. S6B), whereas spindle positioning was randomized in those HsSAS-6-depleted cells with an asymmetrical bipolar spindle (Fig. 6D; supplementary material Fig. S6B). We conclude that impaired centriole formation can generally cause spindle positioning defects in human cells.

Discussion

We undertook a structure–function analysis of CPAP and demonstrated that alterations in proteins that resemble MCPH CPAP patient mutations compromise centriole formation in human cells. In addition, using adhesive micropatterns, we revealed that such defects lead to randomization of spindle position. Furthermore, we established that the MCPH protein STIL is also essential for centriole formation and proper spindle position. Our findings lead us to propose that mutations in CPAP and STIL might cause MCPH because of aberrant centriole formation and thus spindle positioning in progenitor cells during brain development.

Structure–function analysis of CPAP

By depleting endogenous CPAP and concomitantly expressing various deletion and mutant fusion proteins, we clarified the contribution of different protein domains to CPAP function. Thus, we established that the fourth coiled-coil domain (CC4) is

Table 1. Frequency of different spindle configurations

	Spindle configuration				
Cell type	Symmetric bipolar	Asymmetric bipolar	Monopolar	Multipolar	*n*
Control	95.2 (%)	0.0	2.4	2.4	85
CPAP siRNA	18.7	22.5	58.8	0.0	80
GFP–CPAP FL	95.0	1.7	0.0	3.3	60
GFP–CPAP EV	73.3	16.7	8.3	1.7	60
GFP–CPAP ΔTCP	11.7	45.0	43.3	0.0	60
STIL siRNA	9.6	38.5	40.4	11.5	52

Frequency of bipolar symmetric, bipolar asymmetric and monopolar spindles in control HeLa cells, in HeLa cells depleted of CPAP by siRNAs, as well as in HeLa cells treated with CPAP RNAi and expressing RNAi-resistant GFP–CPAP full-length (FL), E1235V (EV) or ΔTCP. Frequencies are also reported for cells depleted of STIL by siRNAs.

both necessary and sufficient for targeting to centrioles. This region is also needed for CPAP homodimerization (Zhao et al., 2010), raising the possibility that CPAP self-interaction is crucial for centriole targeting. We found that, in contrast to full-length CPAP, a fusion protein lacking CC4 does not sustain overly long centrioles or centriole formation, suggesting that CPAP must homodimerize or be targeted to centrioles to be functional. We also established that the PN2-3 and the SAC domains, although dispensable for centriolar targeting, are essential for excessive centriole elongation and centriole formation, possibly because they mediate interaction with tubulin dimers (Cormier et al., 2009). Furthermore, we uncovered that the TCP domain, to which no function had been ascribed previously, is also dispensable for centriolar targeting but essential for CPAP activity. It will be interesting to uncover the mechanisms by which this evolutionarily conserved domain exerts its activity.

FRAP analysis with a functional GFP–CPAP fusion protein indicates that CPAP, residing at or near centrioles, exchanges with the cytoplasmic pool of the protein. This is in contrast to the situation in *C. elegans*, where GFP–SAS-4 does not exchange substantially with the cytoplasmic pool after its incorporation into centrioles (Leidel and Gönczy, 2003). It is possible that the dynamics of this protein family differs across evolution, which would not be all that surprising given the large divergence at the amino acid level between SAS-4 and CPAP (Leidel and Gönczy, 2003). In this respect, it will be informative to assess the kinetics of *Drosophila* Sas-4, which is more closely related to CPAP than it is to SAS-4 (Basto et al., 2006).

STIL is essential for centriole formation

It has been proposed that the MCPH7 protein STIL is a relative of *Drosophila* Ana2 and of *C. elegans* SAS-5 (Stevens et al., 2010a), which are essential for centriole formation in these invertebrate systems (Dammermann et al., 2004; Delattre et al., 2004; Stevens et al., 2010a). STIL homologues localize to the centrosome in mice and zebrafish (Izraeli et al., 1999; Pfaff et al., 2007), but whether this family of proteins is needed for centriole formation in vertebrate systems has not been previously addressed. Here, using siRNA-mediated inactivation, we establish that STIL is required for centriole formation in human cells. In *C. elegans*, SAS-5 associates with SAS-6 (Leidel et al., 2005), which is a crucial component for initiating centriole formation (reviewed by Strnad and Gönczy, 2008). In *Drosophila*, combined overexpression of Ana2 and Sas-6, but not of Sas-6 alone, results in the formation of structures that resemble the cartwheel that is present at the onset of centriole

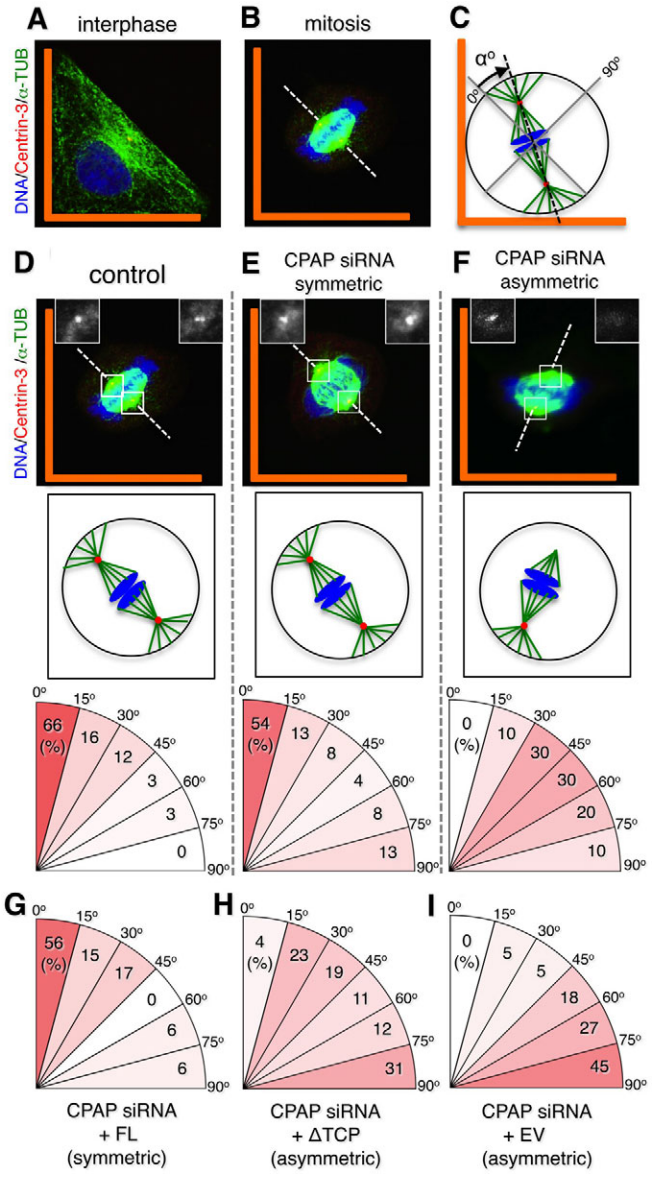

Fig. 5. CPAP is required for proper spindle positioning in human cells. (**A**,**B**) Representative interphase (A) and mitotic (B) HeLa cells on an L-shaped fibronectin micropattern (orange), stained with antibodies against centrin-3 (red) and α-tubulin (green); DNA is shown in blue. Note that the cell spreads along the L-shaped micropatterned fibronectin substrate during interphase and orients along the hypotenuse of the L-shape during mitosis (the dashed lines indicates the position of the mitotic spindle). (**C**) Schematic representation of mitotic spindle geometry on the L-shaped micropattern. The spindle is shown in green, centrosomes in red and chromosomes in blue. Spindle position was determined during metaphase–early anaphase as an angle, as depicted, with 0° being defined as parallel to the hypotenuse of the L. (**D–F**) Synchronized HeLa cells either untreated (D), or treated with siRNAs against CPAP (E,F) plated on L-shaped fibronectin micropatterns (orange) and stained with antibodies against centrin-3 (in red in the low magnification merged images and in black and white in the approximately twofold magnified insets) and α-tubulin (green); DNA is shown in blue. The dashed lines indicate the position of mitotic spindles. Second row from top: schematic view of mitotic configurations. Third row from top: frequency of angular distributions of spindle orientations in 15° increments, with the shading indicative of the frequency in each class (n=32 for control, n=24 for CPAP siRNA symmetric, n=10 for CPAP siRNA asymmetric). See supplementary material Fig. S6A for statistical analysis. (**G–I**) Frequency of angular distributions of spindle orientations as described above for cells treated with siRNAs against CPAP and expressing RNAi-resistant GFP-FL (G; n=34), GFP–ΔTCP (H; n=26) or GFP–CPAP E1235V (I; n=22). Note that spindle position in cells expressing either GFP–ΔTCP or GFP–CPAP E1235V and that assembled a symmetrical bipolar spindle was similar, but not identical, to that of the wild type (data not shown). Note also that asymmetrical spindles in cells expressing GFP–CPAP E1235V do not appear to stem from the presence of longer centrioles, because asymmetrical spindles were observed in such cells irrespective of overly long centrioles being present. See supplementary material Fig. S6A for statistical analysis.

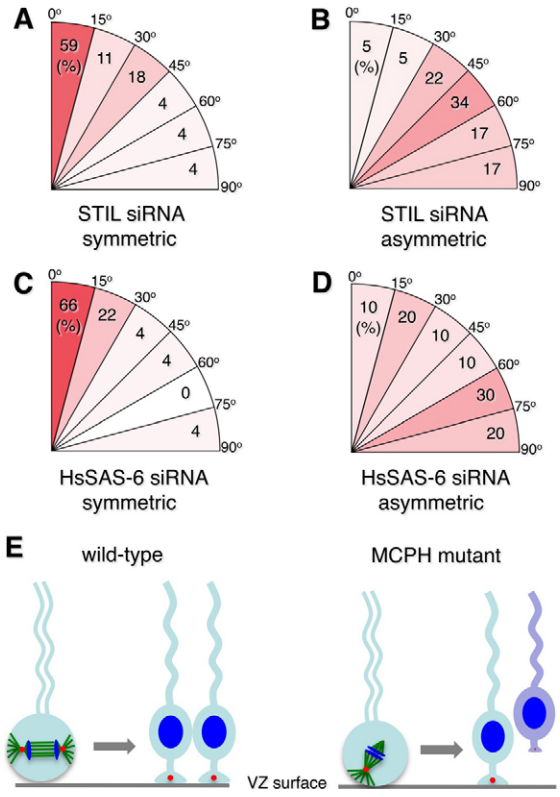

Fig. 6. The MPCH protein STIL and proper centriole formation are required for correct spindle positioning in human cells. (**A–D**) Synchronized HeLa cells treated with siRNAs against STIL (symmetric, A; asymmetric, B), or siRNAs against HsSAS-6 (symmetric, C; asymmetric, D), plated on L-shaped, fibronectin micropatterns and stained with antibodies against centrin and α-tubulin and counterstained for DNA. Percentages of angular distribution of spindle positions every 15° are shown, with the shading being indicative of the frequency of each class (n=27 for STIL siRNA symmetric, n=18 for STIL siRNA asymmetric, n=27 for HsSAS-6 siRNA symmetric, n=10 for HsSAS-6 siRNA asymmetric). See supplementary material Fig. S6B for statistical analysis. (**E**) Speculative model suggesting how defective CPAP or STIL function reduces the pool of neuroepithelial progenitors in MCPH patients. Normally (left), progenitor cells predominantly divide symmetrically during early brain development, with the spindle being positioned parallel to the ventricular surface, thus maintaining the progenitor cell pool. When CPAP or STIL function is altered in MCPH patients (right), centriole formation is defective, which sometimes results in the spindle being positioned perpendicular to the ventricular surface, which results in a reduction of the progenitor pool during early brain development.

formation (Stevens et al., 2010b). Given that SAS-6 proteins are crucial for cartwheel assembly (Kitagawa et al., 2011), all these findings raise the possibility that STIL somehow helps HsSAS-6 to initiate centriole formation. Regardless of the actual underlying mechanism, our findings lend support to the notion that SAS-5–Ana2–STIL is an evolutionarily conserved module crucial for centriole formation.

Spindle positioning defects and the root of MCPH

MCPH is thought to result from the depletion of progenitor cells from the ventricular zone during the initial stage of lateral expansion during brain development (reviewed by Thornton and Woods, 2009). Previous work in the developing mouse brain indicated that depletion of the MCPH protein ASPM results in spindle positioning defects (Fish et al., 2006), although it was shown more recently that mutations in mouse *Aspm* do not affect this process (Pulvers et al., 2010). This apparent discrepancy might be explained by residual function of the mutant proteins or else compensatory mechanisms upon chronic inactivation that are not operating upon acute depletion mediated by RNAi. Regardless, depletion of ASPM in human cells results in severe defects during mitosis, including spindle positioning (Higgins et al., 2010). Together, these results suggest that conclusions drawn from tissue culture cells can shed light on the understanding of the disease situation, and also that spindle positioning defects might contribute to the etiology of MCPH. However, whether inactivation of other MCPH proteins with apparently distinct cellular function also results in spindle positioning defects was not known before our study.

We utilized microfabricated chips as a novel assay for analyzing spindle positioning upon depletion of MCPH components or in conditions mimicking the mutations in MCPH patients. This allowed us to establish that impairment of CPAP or STIL, two MCPH proteins that are required for centriole formation, and thus have a function distinct from that of ASPM, results in randomized spindle position in human cells. Although it remains to be determined whether similar defects occur in human neuronal progenitor cells, we note that spindle positioning defects are also observed in *Drosophila* Sas-4 mutant neuroblasts (Basto et al., 2006). The results to date are compatible with the view that spindle positioning defects lead to aberrant divisions in the ventricular zone of affected patients and thus could explain the depletion of the progenitor cell pool (Fig. 6E). How might aberrant spindle positioning result in the loss of neuronal progenitors? Conceivably, this could be due to premature asymmetrical divisions, which deplete the pool of progenitor cells, as proposed for instance upon depletion of ASPM by RNAi (Fish et al., 2006). Alternatively, aberrant spindle positioning could result in the scattering of progenitor cells away from the ventricular zone, as observed in the developing mouse brain following LGN inactivation or PINS overexpression, which ultimately accelerates depletion of the progenitor pool (Konno et al., 2008). In addition, other mitotic defects due to impaired CPAP or STIL function might contribute to the disease, perhaps because neuronal progenitors are more sensitive to such perturbations than most other cells.

In conclusion, our findings raise the possibility that different MCPH components, although required for distinct cell biological processes, all affect brain development because their impairment leads to a randomization of spindle position in progenitor cells. In addition, the centrosomal protein Cep152 is also needed for centriole formation and is another MCPH component (Blachon et al., 2008; Guernsey et al., 2010). Therefore, it is tempting to speculate that alterations in other components known to be essential for centriole formation, provided that they are not detrimental to life, might be at the root of poorly tractable sporadic cases of microcephaly.

Materials and Methods

Molecular biology

Full-length and fragments of a cDNA encoding CPAP were cloned into pEGFP-C3 (Clonetech) for transient transfection. Four silent nucleotide changes were introduced in the siRNA target region (nucleotides 2862–2880, new sequence: 5′-AGAGTTAGCTAGGATCGAAGA-3′) to generate RNAi-resistant constructs. From this modified cDNA, CPAP E1235V and the deletion mutants were

generated. These constructs were then cloned into pENTR 1A (Invitrogen) and subsequently transferred into pEBTet-EGFP [modified from Bach et al. (Bach et al., 2007) for inducible expression].

Cell lines, fluorescence-activated cell sorting analysis and RNA interference

U2OS cells expressing GFP-centrin-1 (Piel et al., 2000), regular U2OS cells and HeLa cells were cultured in high-glucose DMEM with GlutaMAX (Invitrogen) supplemented with 10% fetal calf serum (FCS) in a humidified 5% CO_2 atmosphere at 37℃. To generate inducible cell lines, cells were transiently transfected with pEBTet-EGFP-CPAP full-length or mutants at 80–90% confluency. After 24 hours, cells were exposed to selective medium containing 1 μg/ml puromycin, which led to substantial death of non-transfected cells over 4–5 days. After amplification under selective conditions for 1–2 weeks, cells were frozen in 10% DMSO and stored at −80℃. Expression was induced using 1 μg/ml doxycyclin.

For fluorescence-activated cell sorting (FACS) analysis, cells were synchronized at the G1–S transition by a double thymidine block. Cells were incubated with 2 mM thymidine for 18 hours, released for 6 hours and again incubated with thymidine for 18 hours. Cells were then released and samples taken at various times after the release, stained with propidium iodide and the DNA content measured by flow cytometry (FACScan, BD Biosciences).

For RNAi experiments, ~100.000 cells were seeded on 18 mm sterile glass coverslips in six-well plates. 6 μl of 20 μM siRNA in 100 μl OptiMEM medium (Invitrogen) and 4 μl of Lipofectamine RNAiMAX (Invitrogen) in 100 μl OptiMEM were incubated in parallel for 5 minutes, mixed for 15 minutes and then added to 2 ml medium per well. The transfected cells were analyzed after 72 hours. Double stranded siRNA oligonucleotides were synthesized with 3′-UU overhangs with the sequence 5′-AGAAUUAGCUCGAAUAGAA-3′ (CPAP siRNA; Dharmacon), 5′-UCUAUAUCAUGGCCGACAA-3′ (control siRNA; Dharmacon) and 5′-AACGUUUACCAUACAAAGAAA-3′ (STIL siRNA; Qiagen). siRNA against HsSAS-6 was as described previously (Strnad et al., 2007).

To assess the efficacy of STIL siRNA, total RNA from HeLa cells was isolated with the RNeasy kit (Qiagen) and first-strand cDNA synthesized using the RevertAid™ first strand cDNA synthesis kit (Fermentas). The following paired primers were used for the PCR reaction: *STIL* (5′-tggagatttcatctacttac-3′ and 5′-gaagtgatatgaactcttag-3′), *GAPDH* (5′-caaggtcatccatgacaactttg-3′ and 5′-gtccaccaccctgttgctgtag-3′).

For plasmid transfections, cells were seeded at 80–90% confluency. 1 μg of plasmid DNA in 50 μl OptiMEM and 2 μl of Lipofectamine 2000 (Invitrogen, Carlsbad, CA) in 50 μl were incubated in parallel for 5 minutes, mixed for 20 minutes and added to each well.

Fluorescence recovery after photobleaching

Fluorescence recovery after photobleaching (FRAP) was performed on a Zeiss LSM700 (Fig. 1F) or on a Leica TCS SP2 (Fig. 1G–H) inverted confocal microscope with a 63× oil immersion objective in an equilibrated chamber in 5% CO_2 at 37℃. The medium was replaced by pre-warmed colorless DMEM (Invitrogen) supplemented with FCS before the experiment. A small region of interest around the centrosomal GFP signal was bleached three times with maximum laser intensity. Three *z*-stacks 1 μm apart were then recorded and the maximum intensity projection image used for analysis (Fig. 1F), or a single confocal section was recorded (Fig. 1G,H). The centrosomal signal could usually be followed without refocusing for 3 minutes. For later time points, owing to centrosome movements, the imaging plane with highest centrosomal fluorescence had to be identified by refocusing.

For Fig. 1F, signal intensities at the core of centrosomes were measured using ImageJ, by determining the mean signal intensity within a 2×2 μm square minus the mean signal intensity of a 250-nm-wide stripe surrounding this square, divided by the background value outside the bleached region to account for potential photobleaching during the recovery period (see Dammermann et al., 2008). For Fig. 1G and H, signal intensities were measured within the bleached region, and the background value subtracted.

Immunoblotting and indirect immunofluorescence

To determine endogenous and exogenous CPAP levels, cells were lysed in 50 mM HEPES (pH 7.4), 250 mM NaCl, 5 mM EDTA, 1% NP-40 and protease inhibitors (P8340; Sigma-Aldrich) by three freeze-thaw cycles in liquid nitrogen, and then centrifuged at 16,000 ***g*** for 10 minutes to remove cell debris. Protein concentration was determined by the Bradford method. Lysate (80 μg) was resolved by SDS-PAGE on a 4–15% gradient gel and immunoblotted on Immobilon-P transfer membrane (Millipore Corporation). Primary antibodies were rabbit anti-CPAP (1:500 dilution) (Kohlmaier et al., 2009), and mouse anti-α-tubulin (DM1a; Sigma; 1:1000) diluted in 5% non-fat dry milk in PBS. Secondary antibodies were HRP-conjugated anti-rabbit or mouse IgG (Promega: 1:5000). Washes were in PBS containing 0.02% Tween (PBST). The signal was detected as chemiluminescence (Roche or Pierce). The signal intensity of a band was measured using ImageJ and the background was subtracted to determine the actual value. Quantification and statistical analysis of the relative levels of exogenous GFP–CPAP fusion proteins normalized to α-tubulin were performed in five experiments.

For immunofluorescence, cells were fixed in −20℃ methanol for 10 minutes and washed in PBS–0.05% Triton X-100. After blocking in 1% BSA in PBS–0.1% Triton X-100 (PBX-100) for 1 hour, cells were incubated with primary antibodies overnight at 4℃. Following three washes in PBX-100 for 5 minutes each, cells were incubated with secondary antibodies and 1 μg/ml Hoechst 33258 for 1 hour at room temperature, washed four times for 5 minutes in PBS-X-100 and mounted. Primary antibodies were rabbit anti-CPAP (1:1000) (Kohlmaier et al., 2009), mouse anti-α-tubulin (DM1a, Sigma; 1:250), mouse anti-γ-tubulin (GTU88, Sigma; 1:2000), mouse '20H5' anti-centrin-2 (1:1000; a gift from Jeff Salisbury), rabbit anti-centrin-3 (1:2000; a gift from Michel Bornens), rabbit anti-C-Nap1 (1:2000; a gift from Erich Nigg), rabbit anti-HsSAS-6 (1:200) (Strnad et al., 2007) and rabbit anti-GFP (1:200; a gift from Viesturs Simanis). Secondary antibodies were Alexa-Fluor-488-coupled anti-mouse (1:500) and Alexa-Fluor-568-coupled anti-rabbit (1:500). Confocal images were taken on a Leica TCS SP2 inverted microscope using a 63× oil immersion objective (Zeiss, Germany). Confocal sections of relevant structures were taken at 0.2–0.4 μm intervals and maximum intensity projected using the Leica LCS Lite software (Leica Microsystems, Germany). Images were processed in Adobe Photoshop.

Spindle orientation assay with CYTOO chips

HeLa cells expressing GFP–CPAP full-length (FL), ΔTCP or EV plasmids were treated with CPAP siRNAs for ~72 hours in total. Approximately 15 hours after siRNA treatment, cells were induced with doxycycline, and ~28 hours thereafter synchronized using 2 mM thymidine for 20 hours. Cells were then released from the thymidine block, trypsinized and plated on L-shaped, fibronectin-micropatterned chips (CYTOO SA, Grenoble, France). Approximately 60,000 cells were placed on a CYTOO chip in a 35 mm culture dish. After 1 hour, floating cells not attached to the micropatterns were removed by gently washing with medium. After ~8 hours, cells were fixed with PTEMF buffer (20 mM PIPES, pH 6.8, 10 mM EGTA, 1 mM $MgCl_2$, 0.2% Triton X-100, 4% formaldehyde) and stained with antibodies against GFP and α-tubulin or centrin-3 as described above. HeLa cells treated with siRNAs directed against CPAP or STIL were handled in a similar manner, except that doxycycline was not added.

Acknowledgements

We thank Sachin Kotak for advice with CYTOO chips, Michel Bornens, Erich Nigg, Jeff Salisbury and Viesturs Simanis for their gift of antibodies and cells, as well as Sachin Kotak, Alexey Khodjakov and Virginie Hachet for comments on the manuscript.

Funding

This work was supported by post-doctoral fellowships from the JSPS to D.K.; European Molecular Biology Organisation [grant number ALTF-667-2007 to D.K.]; the Fundación Ramón Areces to F.R.B.; Oncosuisse [grant number OCS KLS 02024-02-2007 to P.G.]; and the European Research Council [grant number AdG 233335 to P.G.].

Supplementary material available online at
http://jcs.biologists.org/lookup/suppl/doi:10.1242/jcs.089888/-/DC1

References

Bach, M., Grigat, S., Pawlik, B., Fork, C., Utermohlen, O., Pal, S., Banczyk, D., Lazar, A., Schomig, E. and Grundemann, D. (2007). Fast set-up of doxycycline-inducible protein expression in human cell lines with a single plasmid based on Epstein-Barr virus replication and the simple tetracycline repressor. *FEBS J.* **274**, 783-790.

Basto, R., Lau, J., Vinogradova, T., Gardiol, A., Woods, C. G., Khodjakov, A. and Raff, J. W. (2006). Flies without centrioles. *Cell* **125**, 1375-1386.

Blachon, S., Gopalakrishnan, J., Omori, Y., Polyanovsky, A., Church, A., Nicastro, D., Malicki, J. and Avidor-Reiss, T. (2008). *Drosophila* asterless and vertebrate Cep152 Are orthologs essential for centriole duplication. *Genetics* **180**, 2081-2094.

Bobinnec, Y., Khodjakov, A., Mir, L. M., Rieder, C. L., Edde, B. and Bornens, M. (1998). Centriole disassembly in vivo and its effect on centrosome structure and function in vertebrate cells. *J. Cell Biol.* **143**, 1575-1589.

Bond, J., Roberts, E., Springell, K., Lizarraga, S. B., Scott, S., Higgins, J., Hampshire, D. J., Morrison, E. E., Leal, G. F., Silva, E. O. et al. (2005). A centrosomal mechanism involving CDK5RAP2 and CENPJ controls brain size. *Nat. Genet* **37**, 353-355.

Cormier, A., Clement, M. J., Knossow, M., Lachkar, S., Savarin, P., Toma, F., Sobel, A., Gigant, B. and Curmi, P. A. (2009). The PN2-3 domain of centrosomal P4.1-associated protein implements a novel mechanism for tubulin sequestration. *J. Biol. Chem.* **284**, 6909-6917.

Dammermann, A., Müller-Reichert, T., Pelletier, L., Habermann, B., Desai, A. and Oegema, K. (2004). Centriole assembly requires both centriolar and pericentriolar material proteins. *Dev. Cell* **7**, 815-829.

Dammermann, A., Maddox, P. S., Desai, A. and Oegema, K. (2008). SAS-4 is recruited to a dynamic structure in newly forming centrioles that is stabilized by the gamma-tubulin-mediated addition of centriolar microtubules. *J. Cell Biol.* **180**, 771-785.

Delattre, M., Leidel, S., Wani, K., Baumer, K., Bamat, J., Schnabel, H., Feichtinger, R., Schnabel, R. and Gönczy, P. (2004). Centriolar SAS-5 is required for centrosome duplication in *C. elegans*. *Nat. Cell Biol.* **6**, 656-664.

Fish, J. L., Kosodo, Y., Enard, W., Pääbo, S. and Huttner, W. B. (2006). Aspm specifically maintains symmetric proliferative divisions of neuroepithelial cells. *Proc. Natl. Acad. Sci. USA* **103**, 10438-10443.

Fry, A. M., Mayor, T., Meraldi, P., Stierhof, Y. D., Tanaka, K. and Nigg, E. A. (1998). C-Nap1, a novel centrosomal coiled-coil protein and candidate substrate of the cell cycle-regulated protein kinase Nek2. *J. Cell Biol.* **141**, 1563-1574.

Guernsey, D. L., Jiang, H., Hussin, J., Arnold, M., Bouyakdan, K., Perry, S., Babineau-Sturk, T., Beis, J., Dumas, N., Evans, S. C. et al. (2010). Mutations in centrosomal protein CEP152 in primary microcephaly families linked to MCPH4. *Am. J. Hum. Genet.* **87**, 40-51.

Gul, A., Hassan, M. J., Hussain, S., Raza, S. I., Chishti, M. S. and Ahmad, W. (2006). A novel deletion mutation in CENPJ gene in a Pakistani family with autosomal recessive primary microcephaly. *J. Hum. Genet.* **51**, 760-764.

Higgins, J., Midgley, C., Bergh, A. M., Bell, S. M., Askham, J. M., Roberts, E., Binns, R. K., Sharif, S. M., Bennett, C., Glover, D. M. et al. (2010). Human ASPM participates in spindle organisation, spindle orientation and cytokinesis. *BMC Cell Biol.* **11**, 85.

Hung, L. Y., Tang, C. J. and Tang, T. K. (2000). Protein 4.1 R-135 interacts with a novel centrosomal protein (CPAP) which is associated with the gamma-tubulin complex. *Mol. Cell Biol.* **20**, 7813-7825.

Izraeli, S., Lowe, L. A., Bertness, V. L., Good, D. J., Dorward, D. W., Kirsch, I. R. and Kuehn, M. R. (1999). The SIL gene is required for mouse embryonic axial development and left-right specification. *Nature* **399**, 691-694.

Khodjakov, A. and Rieder, C. L. (2001). Centrosomes enhance the fidelity of cytokinesis in vertebrates and are required for cell cycle progression. *J. Cell Biol.* **153**, 237-242.

Kirkham, M., Müller-Reichert, T., Oegema, K., Grill, S. and Hyman, A. A. (2003). SAS-4 is a *C. elegans* centriolar protein that controls centrosome size. *Cell* **112**, 575-587.

Kitagawa, D., Vakonakis, I., Olieric, N., Hilbert, M., Keller, D., Olieric, V., Bortfeld, M., Erat, M. C., Flückiger, I., Gönczy, P. et al. (2011). Structural basis of the nine-fold symmetry of centrioles. *Cell* **144**, 364-375.

Kleylein-Sohn, J., Westendorf, J., Le Clech, M., Habedanck, R., Stierhof, Y. D. and Nigg, E. A. (2007). Plk4-induced centriole biogenesis in human cells. *Dev. Cell* **13**, 190-202.

Kohlmaier, G., Loncarek, J., Meng, X., McEwen, B. F., Mogensen, M. M., Spektor, A., Dynlacht, B. D., Khodjakov, A. and Gönczy, P. (2009). Overly long centrioles and defective cell division upon excess of the SAS-4-related protein CPAP. *Curr. Biol.* **19**, 1012-1018.

Konno, D., Shioi, G., Shitamukai, A., Mori, A., Kiyonari, H., Miyata, T. and Matsuzaki, F. (2008). Neuroepithelial progenitors undergo LGN-dependent planar divisions to maintain self-renewability during mammalian neurogenesis. *Nat. Cell Biol.* **10**, 93-101.

Kumar, A., Girimaji, S. C., Duvvari, M. R. and Blanton, S. H. (2009). Mutations in STIL, encoding a pericentriolar and centrosomal protein, cause primary microcephaly. *Am. J. Hum. Genet* **84**, 286-290.

Leidel, S. and Gönczy, P. (2003). SAS-4 is essential for centrosome duplication in *C. elegans* and is recruited to daughter centrioles once per cell cycle. *Dev. Cell* **4**, 431-439.

Leidel, S., Delattre, M., Cerutti, L., Baumer, K. and Gönczy, P. (2005). SAS-6 defines a protein family required for centrosome duplication in *C. elegans* and in human cells. *Nat. Cell Biol.* **7**, 115-125.

O'Connell, C. B. and Wang, Y. L. (2000). Mammalian spindle orientation and position respond to changes in cell shape in a dynein-dependent fashion. *Mol. Biol. Cell* **11**, 1765-1774.

Pfaff, K. L., Straub, C. T., Chiang, K., Bear, D. M., Zhou, Y. and Zon, L. I. (2007). The zebra fish cassiopeia mutant reveals that SIL is required for mitotic spindle organization. *Mol. Cell Biol.* **27**, 5887-5897.

Piel, M., Meyer, P., Khodjakov, A., Rieder, C. L. and Bornens, M. (2000). The respective contributions of the mother and daughter centrioles to centrosome activity and behavior in vertebrate cells. *J. Cell Biol.* **149**, 317-330.

Pulvers, J. N., Bryk, J., Fish, J. L., Wilsch-Bräuninger, M., Arai, Y., Schreier, D., Naumann, R., Helppi, J., Habermann, B., Vogt, J., et al. (2010). Mutations in mouse Aspm (abnormal spindle-like microcephaly associated) cause not only microcephaly but also major defects in the germline. *Proc. Natl. Acad. Sci. USA* **107**, 16595-16600.

Schmidt, T. I., Kleylein-Sohn, J., Westendorf, J., Le Clech, M., Lavoie, S. B., Stierhof, Y. D. and Nigg, E. A. (2009). Control of centriole length by CPAP and CP110. *Curr. Biol.* **19**, 1005-1011.

Stevens, N. R., Dobbelaere, J., Brunk, K., Franz, A. and Raff, J. W. (2010a). *Drosophila* Ana2 is a conserved centriole duplication factor. *J. Cell Biol* **188**, 313-323.

Stevens, N. R., Roque, H. and Raff, J. W. (2010b). DSas-6 and Ana2 coassemble into tubules to promote centriole duplication and engagement. *Dev. Cell* **19**, 913-919.

Strnad, P. and Gönczy, P. (2008). Mechanisms of procentriole formation. *Trends Cell Biol.* **18**, 389-396.

Strnad, P., Leidel, S., Vinogradova, T., Euteneuer, U., Khodjakov, A. and Gönczy, P. (2007). Regulated HsSAS-6 levels ensure formation of a single procentriole per centriole during the centrosome duplication cycle. *Dev. Cell* **13**, 203-213.

Tang, C. J., Fu, R. H., Wu, K. S., Hsu, W. B. and Tang, T. K. (2009). CPAP is a cell-cycle regulated protein that controls centriole length. *Nat. Cell Biol.* **11**, 825-831.

Théry, M., Racine, V., Pepin, A., Piel, M., Chen, Y., Sibarita, J. B. and Bornens, M. (2005). The extracellular matrix guides the orientation of the cell division axis. *Nat. Cell Biol.* **7**, 947-953.

Thornton, G. K. and Woods, C. G. (2009). Primary microcephaly: do all roads lead to Rome? *Trends Genet* **25**, 501-510.

Wakefield, J. G., Bonaccorsi, S. and Gatti, M. (2001). The drosophila protein asp is involved in microtubule organization during spindle formation and cytokinesis. *J. Cell Biol.* **153**, 637-648.

Zhao, L., Jin, C., Chu, Y., Varghese, C., Hua, S., Yan, F., Miao, Y., Liu, J., Mann, D., Ding, X. et al. (2010). Dimerization of CPAP orchestrates centrosome cohesion plasticity. *J. Biol. Chem.* **285**, 2488-2497.

Journal of Cell Science